

Dynamic Nuclear Polarization with a Rigid Biradical**

Yoh Matsuki, Thorsten Maly, Olivier Ouari, Hakim Karoui, François Le Moigne, Egon Rizzato, Sevdalina Lyubenova, Judith Herzfeld, Thomas Prisner, Paul Tordo, and Robert G. Griffin*

Dynamic nuclear polarization (DNP) is an approach that can enhance NMR signal intensities of solids and liquids by two to three orders of magnitude. During a DNP experiment, the large Boltzmann polarization of an exogenous or endogenous paramagnetic species, such as a stable free radical, is transferred to the nuclei of interest by microwave (mw) irradiation of the sample at the electron paramagnetic resonance (EPR) frequency. The maximum theoretical enhancement possible is given by the ratio γ_s/γ_I , in which γ_s and γ_I are the gyromagnetic ratios of the electron and the nucleus, respectively. Enhanced nuclear polarization is of considerable interest in a variety of applications ranging from particle physics^[1,2] to structural biology^[3,4] and clinical imaging.^[5] The mechanism that dominates the electron–nucleus polarization transfer depends on the relative sizes of the homogeneous line width, δ , and inhomogeneous breadth, Δ , of the EPR spectrum of the paramagnetic polarizing agent and the nuclear Larmor frequency, ω_{0I} . When $\delta, \Delta < \omega_{0I}$, DNP is

dominated by the solid effect (SE), whereas the cross-effect (CE) is operative when $\Delta > \omega_{0I} > \delta$.^[3]

In general, the largest signal enhancements observed at high magnetic fields (≥ 5 T) are in experiments in which the CE controls the polarization transfer.^[6,7] The underlying mechanism of the CE is a two-step process that involves two electrons with Larmor frequencies ω_{0S1} and ω_{0S2} , and a nucleus with a frequency ω_{0I} . Initially, the EPR transition of one electron is irradiated and nuclear polarization is generated in a subsequent three-spin flip-flop process through transitions such as $|\alpha_{1S}\beta_{2S}\beta_I\rangle \leftrightarrow |\beta_{1S}\alpha_{2S}\alpha_I\rangle$ or $|\beta_{1S}\alpha_{2S}\beta_I\rangle \leftrightarrow |\alpha_{1S}\beta_{2S}\alpha_I\rangle$.^[8–10] Therefore, the CE is optimized when there is a sufficiently strong dipolar coupling between the two electrons, and when the difference between the electron Larmor frequencies approximates the nuclear Larmor frequency ($\omega_{0S1} - \omega_{0S2} \approx \pm \omega_{0I}$). These requirements can be fulfilled more easily within a biradical than among dispersed monoradicals,^[11] and we have demonstrated that the optimal polarizing agent for experiments in glycerol/water is currently the TEMPO-based biradical 1-(TEMPO-4-oxy)-3-(TEMPO-4-amino)propan-2-ol (TOTAPOL; TEMPO = 2,2,6,6-tetramethylpiperidin-1-oxyl; Scheme 1, bottom).^[12] However, at high magnetic fields the effective electron resonance fre-

[*] Dr. Y. Matsuki, Dr. T. Maly, Prof. R. G. Griffin
Francis Bitter Magnet Laboratory and Department of Chemistry
Massachusetts Institute of Technology
Cambridge, MA 02139 (USA)
Fax: (+1) 781-736-2538
E-mail: rgg@mit.edu
Homepage: <http://web.mit.edu/fbml/cmr/griffin-group/index.html>

Dr. Y. Matsuki, Prof. J. Herzfeld
Department of Chemistry, Brandeis University
Waltham, MA 02454 (USA)

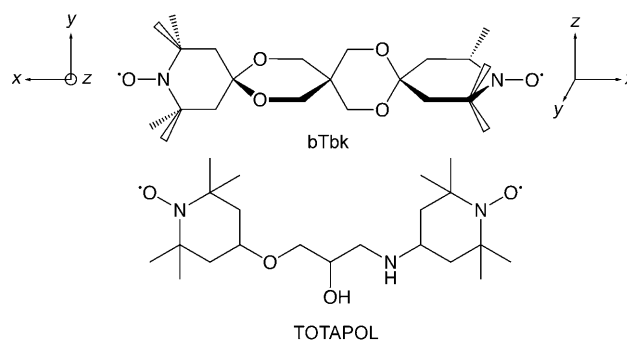
Dr. O. Ouari, Prof. P. Tordo
CNRS-UMR 6517, Chemistry, Biology and Free Radicals
University of Aix-Marseille I and III, Marseille (France)

Dr. H. Karoui, Dr. F. Le Moigne, Dr. E. Rizzato
LCP CNRS-UMR 6264, University of Provence
13397 Marseille Cedex 20 (France)

Dr. S. Lyubenova, Prof. T. Prisner
Institute of Physical and Theoretical Chemistry and
Center for Biomolecular Magnetic Resonance
60438 Frankfurt (Germany)

[**] We thank Sandrine Lambert for technical assistance, and Galia Debelouchina, Albert Smith, Alexander Barnes, and Jean-Pierre Finet for many stimulating discussions. This research was supported by the National Institutes of Health through grants EB002804, EB002026, EB009866, EB001965, and EB001035, and by the EU-Design Study Bio-DNP in Framework 6. T.M. acknowledges receipt of a postdoctoral fellowship from the Deutsche Forschungsgemeinschaft. Y.M. acknowledges partial financial support from the Naito Foundation.

Supporting information for this article is available on the WWW under <http://dx.doi.org/10.1002/anie.200805940>.



Scheme 1. Molecular structure of the two biradicals used in the DNP experiments described herein. The axis systems on each side of bis-TEMPO-bisketal (bTbk) show the direction of the principal g -tensor components of TEMPO for the assumed perfect perpendicular relative orientation.

quency can depend strongly on the molecular orientation with respect to the external magnetic field, and in a biradical the matching condition is controlled by the relative orientations of the electron g tensors. In particular, since the propan-2-ol tether in TOTAPOL is relatively flexible,^[6] the two TEMPO moieties are not constrained in a single relative orientation, and many orientations do not lead to the correct frequency separation. Therefore, a more rigid tether that locks the two

TEMPO moieties in a desirable relative orientation should further increase the enhancement obtained from the polarizing agent.

Herein, we demonstrate the utility of bis-TEMPO-bisketal (bTbk; Scheme 1, top), a biradical consisting of two TEMPO moieties connected with a rigid bisketal tether. This biradical was originally used to inhibit radical polymerization.^[13] In particular, we compare the performance of bTbk and TOTAPOL in DNP experiments under similar experimental conditions.

Earlier studies of a series of TEMPO-based biradicals as polarizing agents in high-field DNP experiments suggested that a conformation in which the two g_{zz} (or g_{yy}) tensor axes of the TEMPO moieties have a dihedral angle of 90° should exhibit improved performance as a result of efficient frequency matching.^[6] This requirement is approximately fulfilled (see below) for bTbk (Scheme 1, top) as a result of the odd number of spiro junctions between the two TEMPO moieties. Specifically, the crystal structure of bTbk shows a dihedral angle between the TEMPO moieties of 82° . Furthermore, a calculated average electron–electron distance of 1.18 nm (see Figure S1 in the Supporting Information) was confirmed by pulsed electron–electron double resonance (PELDOR) measurements (see Figure S2 in the Supporting Information). The dihedral angle restrains the g_{zz} (or g_{yy}) tensor components of the two TEMPO moieties in a perpendicular conformation to ensure a large frequency separation for molecular orientations along these axes. At the same time, the short distance provides the large electron–electron dipolar coupling required for an efficient DNP process.

Initial DNP experiments with bTbk are described in Figure 1. A typical ^{13}C -detected buildup curve of the ^1H -bulk polarization is shown together with spectra recorded with and without microwave irradiation at fields corresponding to the

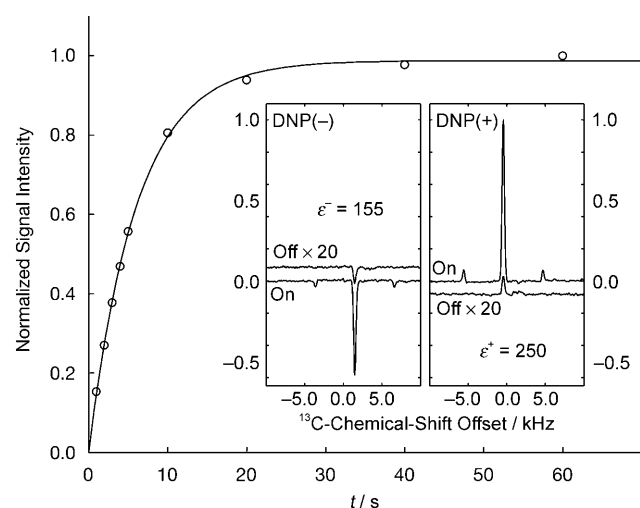


Figure 1. Buildup curve recorded at a magnetic-field position corresponding to DNP(+) for ^1H bulk polarization with bTbk. The ^1H polarization is detected indirectly from the ^{13}C signal of urea through a cross-polarization step. The insets show the mw on and off signals recorded at field positions corresponding to DNP(+) and DNP(-); $T = 94\text{ K}$, $\omega_r/2\pi = 4.8\text{ kHz}$.

maximum positive (DNP(+)) and negative (DNP(-)) DNP enhancements. (The pulse sequence used is given in Figure S3 in the Supporting Information). The ^1H polarization was monitored by transferring the DNP-enhanced ^1H polarization to the ^{13}C nuclei of the urea molecule in a cross-polarization step.^[14,15] At a temperature of 93 K, the buildup time constant τ_B is 7 s, and a steady-state enhancement of $\epsilon^+ = 250$ was observed (Figure 1) at a microwave power of approximately 2.5 W (estimated power at the sample position). This enhancement is larger than that observed with TOTAPOL ($\epsilon^+ = 180$) under identical experimental conditions (solvent, temperature, mw power).

For a more reliable comparison of the two polarizing agents, the enhancement was extrapolated to infinite microwave power ϵ_∞^\pm . This value can be obtained from the dependence of the DNP enhancement on the microwave power according to Equation (1):

$$\frac{1}{\epsilon^\pm} = \frac{1}{\epsilon_\infty^\pm} \left(1 + \frac{1}{aP} \right) \quad (1)$$

in which ϵ^\pm is the steady-state enhancement factor, P is the microwave power, and a is the saturation parameter, which depends on the microwave transmission efficiency and EPR relaxation properties.^[6] Different instrumental conditions, such as the microwave transmission efficiency or EPR relaxation properties, affect ϵ^\pm and a , but not ϵ_∞^\pm .^[6] Nevertheless, the experiments must be performed at similar temperatures for an accurate comparison.

Figure 2 shows the power dependence of the DNP enhancements for bTbk and TOTAPOL. From this relationship, ϵ_∞^\pm can be calculated by using Equation (1). For bTbk and TOTAPOL, the ϵ_∞^\pm values are 325 ± 15 and 227 ± 10 ,

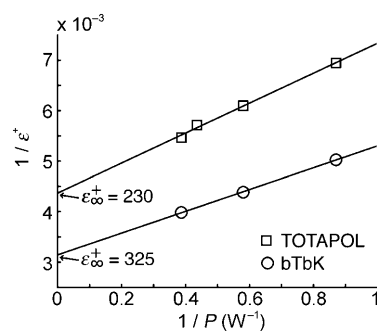


Figure 2. Power dependence of the steady-state DNP enhancement (ϵ^+) for bTbk and TOTAPOL. The experiments with the two polarizing agents were carried out under similar conditions.

respectively. Values of ϵ_∞^\pm for a series of biradicals previously examined in DNP experiments are compared in Table 1. Among the polarizing agents investigated to date, bTbk yields the largest DNP enhancement. The enhancement is approximately 1.4 times larger than that of TOTAPOL.

The DNP process is most efficient if the sample and the polarizing agent are dispersed in a matrix that forms a rigid glass at cryogenic temperatures. For example, mixtures of dimethyl sulfoxide (DMSO)/water (60:40 w/w) or glycerol/

Table 1: DNP enhancement at infinite microwave power for different TEMPO-based biradicals.

Biradical	ϵ_{∞}	Biradical	ϵ_{∞}
BT2E ^[a]	260	BTOXA ^[a]	70
BT3E ^[a]	175	TOTAPOL ^[a,b]	260
BT4E ^[a]	105	TOTAPOL ^[c]	230
BTUrea ^[a]	205	bTbk ^[c]	325

[a] Values taken from reference [6]; [D₆]DMSO/D₂O/H₂O (60:34:6), $T = 90$ K. [b] The previously published value is incorrect; $\epsilon_{\infty} = 260$ is the correct value. [c] Measurements made in the current study; [D₆]DMSO/D₂O/H₂O (77:17:6), $T = 93$ K.

water (60:40 w/w) form rigid glass matrices at 90 K regardless of the cooling rate.^[3,4,16,17] The ability of the solvent to form a glass is important in DNP experiments, because glass formation ensures a homogeneous dispersion of the polarizing agent in the sample, and the solvent can concurrently act as a cryoprotectant. However, in the case of bTbk, the main factor that presently limits its applicability in DNP experiments with biological samples is its sparse solubility in media such as glycerol/water (60:40), which is currently the solvent mixture of choice for DNP experiments on proteins. Although bTbk is soluble in small amounts in DMSO/water (60:40), another mixture used frequently for DNP, its solubility is greater at higher DMSO concentrations. However, DMSO requires a minimum water content of 23 % for successful glass formation at 90 K. Therefore, all experiments reported herein were performed with a 77:23 DMSO/water mixture.

The decreased water content had a dramatic impact on the observed enhancements. In measurements of ϵ_{∞}^{\pm} for TOTAPOL in different solvent matrices with a DMSO content of 50, 64, and 77 %, we observed that the ϵ_{∞}^{\pm} value for 50:50 and 64:36 mixtures of DMSO/water are similar ($\epsilon_{\infty}^{\pm} \approx 260$), whereas the observed enhancement is significantly lower at a water content of 23 % ($\epsilon_{\infty}^{\pm} \approx 230$; see Table 1). This decrease is most likely due to the suboptimal glass-forming properties of the 77:23 DMSO/water mixture. Nevertheless, in this solvent matrix a maximum enhancement of $\epsilon_{\infty}^{\pm} = 325$ was observed for bTbk: an increase of 40 % if the performance is compared with that of TOTAPOL under identical experimental conditions ($\epsilon_{\infty}^{\pm} = 230$ for TOTAPOL). If the ϵ_{∞}^{\pm} values are compared under optimal conditions for bTbk and TOTAPOL, then the increase is 25 % ($\epsilon_{\infty}^{\pm} = 260$ for TOTAPOL in 60:40 DMSO/water). Taken together, these results suggest that still greater DNP enhancements can be expected for a water-soluble form of bTbk.

Since the gyrotron is a fixed-frequency oscillator (operating at 139.662 GHz), the optimum field position for the DNP effect is determined by sweeping the magnetic field, B_0 , and recording the DNP enhancement for each field position. This process yielded the field-dependent DNP enhancement profile in Figure 3 (bottom). Besides identifying the fields for maximum enhancement (DNP(+)) and DNP(-)), the DNP profile provides other important information that can lead to possible improvement of the performance of the polarizing agent.

The DNP enhancement profile is closely related to the high-field EPR spectrum, which is shown for bTbk in Figure 3

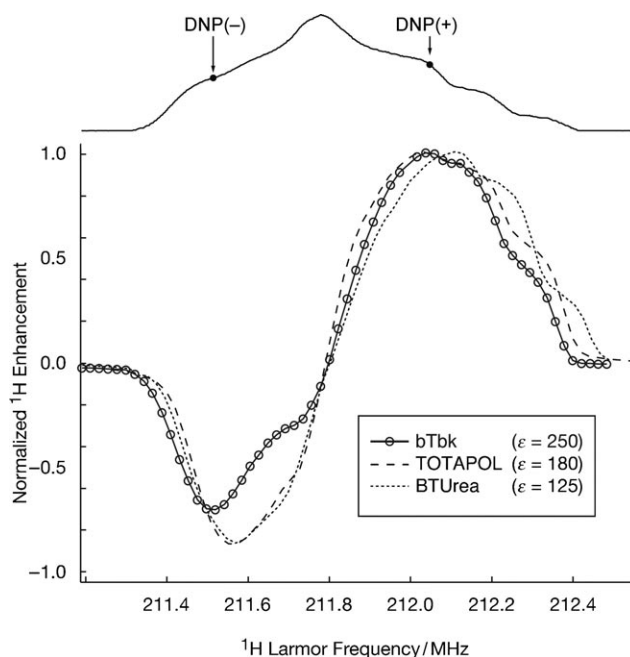


Figure 3. Field dependence of the DNP enhancement profiles and EPR spectrum of bTbk. Top: 140 GHz echo-detected EPR spectrum of bTbk in DMSO/H₂O (77:23); $T = 20$ K, $t_p(\pi/2) = 60$ ns, $\tau = 300$ ns. Bottom: ¹H-detected DNP field profile of bTbk (solid line), TOTAPOL (dashed line), and BTUrea (dotted line); $T = 94$ K, $t_p(\pi/2) = 3$ μ s, $\omega_r/2\pi = 4.8$ kHz. The three enhancement profiles were recorded under similar experimental conditions and are normalized to the maximum positive enhancement. The individual data points are included for bTbk. Similar data were recorded for TOTAPOL and BTUrea; the points are not included on the plots to enable the curves to be distinguished easily. The enhancement factors for bTbk, TOTAPOL, and BTUrea under optimal experimental conditions are given in the box.

(top). Since the electron–electron dipolar coupling is relatively small (ca. 30 MHz) when compared to the breadth of the EPR spectrum, the line shape resembles that of a monomeric nitroxide-based radical at high fields and is dominated by the large anisotropy of the g and the ¹⁴N hyperfine tensors. As the overall inhomogeneous spectral width at 140 GHz is $\Delta \approx 640$ MHz, the CE is the dominant DNP mechanism. In our current DNP instrument, the microwave excitation bandwidth is in the range of a few megahertz, and is small relative to the inhomogeneous breadth of the EPR spectrum, Δ . Hence, only a small portion of the EPR spectrum is excited by the microwave radiation. The portion of the spectrum that is excited corresponds to a particular set of molecular orientations. This phenomenon is referred to as “orientation selection” and is well-known in EPR and electron–nuclear double resonance (ENDOR) spectroscopy.^[18,19] For nitroxide-based radicals, orientation selection is facilitated by the large anisotropy of the g and the ¹⁴N hyperfine tensors ($g_{xx} = 2.00980$, $g_{yy} = 2.00622$, $g_{zz} = 2.00220$, $A_{xx} = 17.0$, $A_{yy} = 20.5$, $A_{zz} = 95.9$ MHz for TEMPO^[20]). Furthermore, among the excited spins, only those that satisfy the matching condition $\omega_{0S1} - \omega_{0S2} \approx \pm \omega_{0I}$ contribute significantly to the DNP effect.^[9,10] Thus, for an inhomogeneously broadened EPR line with $\delta < \omega_{0I} < \Delta$, this

two-step process (orientation selection and frequency matching) governs the field dependence of the DNP effect.

The field-dependent DNP-enhancement profile of bTbk (Figure 3, bottom) shows a maximum positive enhancement at a field position corresponding to an ^1H Larmor frequency of 212.058 MHz (DNP(+)) and a maximum negative enhancement at 211.516 MHz (DNP(-)). These values are separated by 542 kHz (357 MHz for e^-). The zero crossing occurs at approximately 211.8 MHz, which coincides with the maximum absorption in the EPR spectrum (g_{yy} -tensor component of TEMPO).

The DNP-enhancement profile recorded for bTbk shows a pronounced asymmetry across the EPR line. This asymmetry can be described conveniently by the ratio of the maximum negative and positive enhancements, $\varepsilon^-/\varepsilon^+$, which is 0.62 for bTbk (Figure 3, bottom, solid line). The same asymmetry is observed if the ^1H polarization is measured through indirect ^{13}C detection, which gives enhancement factors of $\varepsilon^+ = 250$ and $\varepsilon^- = 155$ (see insets in Figure 1). This asymmetry of the enhancement profile observed for bTbk is more pronounced than for previously studied biradicals, including TOTAPOL and BTUrea (two TEMPO units with a urea tether), for which a smaller asymmetry of $\varepsilon^-/\varepsilon^+ = 0.84$ was observed (Figure 3).^[12] Furthermore, other TEMPO-based biradicals, such as BT2E (two TEMPO units with a bis(ethylene glycol) tether) showed a similar asymmetry factor of approximately 0.8,^[12] whereas the DNP-enhancement profile for monomeric TEMPO is almost symmetrical ($\varepsilon^+/\varepsilon^- \approx 1$).^[21,22] These observations suggest that the asymmetry is an intrinsic feature of TEMPO-based biradicals, and that the extent of the observed asymmetry is a result the flexibility/rigidity of the connecting tether and the relative orientation of the two TEMPO rings. Numerical simulations are currently in progress to investigate this behavior in more detail.

In conclusion, our experiments demonstrate the superior performance of the biradical bTbk over that of other TEMPO biradicals used in DNP experiments. The enhancement factors observed with bTbk are about 1.4 times those observed with TOTAPOL under identical experimental conditions. However, owing to its limited solubility, bTbk requires the use of a modified solvent matrix with a lower water content. The use of this solvent mixture compromises the DNP efficiency and limits the applicability of bTbk to biological systems that require glycerol/water matrices. The larger enhancements observed under these suboptimal conditions provide motivation for the development of water-soluble bTbk derivatives as well as other polarizing agents with strong e^-e^- dipole couplings, rigid tethers, and g tensors with the correct relative orientation.

Experimental Section

Synthesis: The biradical bTbk was synthesized in a two-step sequence in 35% overall yield. The bispiroketal skeleton was obtained by treating pentaerythritol (0.87 g, 6.4 mmol) with 2,2,6,6-tetramethyl-4-piperidone (2.00 g, 12.8 mmol) in the presence of *p*-toluenesulfonic acid (2.21 g, 12.8 mmol) in toluene at reflux. The biradical bTbk was obtained as orange crystals by oxidation of the corresponding diamine

at 0°C with *m*-chloroperbenzoic acid (1.5 equiv) in CH_2Cl_2 . See the Supporting Information for a detailed experimental procedure and characterization.

Sample preparation: For the DNP experiments, 9 mm solutions of bTbk or TOTAPOL in $[\text{D}_6]\text{DMSO}/\text{D}_2\text{O}/\text{H}_2\text{O}$ (77:17:6) were prepared. The small amount of H_2O (6% for all samples) is required to optimize the diffusion of the local DNP-enhanced nuclear polarization to neighboring nuclei. For matrix studies, 9 mm solutions of TOTAPOL in $[\text{D}_6]\text{DMSO}/\text{D}_2\text{O}/\text{H}_2\text{O}$ (64:30:6) and $[\text{D}_6]\text{DMSO}/\text{D}_2\text{O}/\text{H}_2\text{O}$ (50:44:6) were also prepared. All DNP samples contained ^{13}C -urea (2M) to optimize detection of the NMR signal. The high concentration facilitates observation of the microwave off signal (no DNP enhancement) in a reasonable time period. A 2 mm solution of bTbk in $\text{DMSO}/\text{H}_2\text{O}$ (77:23) was prepared for EPR measurements. All solvent mixtures are given in weight percentage.

DNP experiments: DNP experiments were performed on a custom-designed DNP NMR spectrometer by using a triple-resonance cryogenic magic angle spinning probe (e^- , ^1H , and ^{13}C) with a commercial 2.5 mm rotor stator (Revolution NMR Inc.). The spectrometer operates at a magnetic field of 5 T, which corresponds to a Larmor frequency of 140 GHz for e^- and 211 MHz for ^1H . The enhanced ^1H polarization was detected indirectly through observation of the cross-polarization ^{13}C NMR spectrum. The high-power microwave radiation was generated by a gyrotron operating at a frequency of 139.662 GHz.^[21,23,24] A gyrotron is a vacuum electron device capable of producing high-power (> 10 W) millimeter waves. The DNP sample was placed in a 2.5 mm sapphire rotor. The 5 T superconducting magnet was equipped with a superconducting sweep coil so that the field could be swept over ± 750 G to record the DNP field profile, and the magnetic field could be adjusted for maximum enhancement.

EPR experiments: EPR experiments were performed on a previously described^[18,21] custom-designed high-field EPR spectrometer operating at a microwave frequency of 139.504 GHz. The sample, with a volume of approximately 250 nL, was placed in a Suprasil quartz tube with an outer diameter of 0.55 mm. EPR spectra were recorded by using a two-pulse echo sequence ($\pi/2-\tau-\pi-\tau$ -echo) by integrating the echo intensity while sweeping the magnetic field. Detailed experimental conditions are given in the legend for Figure 3. For accurate field measurements, the spectrometer was equipped with a field/frequency lock system.^[25]

Received: December 5, 2008

Revised: April 7, 2009

Published online: June 2, 2009

Keywords: biradicals · dynamic nuclear polarization · EPR spectroscopy · polarizing agents · solid-state NMR spectroscopy

- [1] S. T. Goertz, *Nucl. Instrum. Methods Phys. Res. Sect. A* **2004**, 526, 28.
- [2] R. A. Wind, M. J. Duijvestijn, C. van der Lugt, A. Manenschijn, J. Vriend, *Prog. Nucl. Magn. Reson. Spectrosc.* **1985**, 17, 33.
- [3] T. Maly, G. T. Debelouchina, V. S. Bajaj, K.-N. Hu, C.-G. Joo, M. L. Mak-Jurkauskas, J. R. Sirigiri, P. C. A. van der Wel, J. Herzfeld, R. J. Temkin, R. G. Griffin, *J. Chem. Phys.* **2008**, 128, 052211.
- [4] A. B. Barnes, G. De Paëpe, P. C. A. van der Wel, K. N. Hu, C. G. Joo, V. S. Bajaj, M. L. Mak-Jurkauskas, J. R. Sirigiri, J. Herzfeld, R. J. Temkin, R. G. Griffin, *Appl. Magn. Reson.* **2008**, 34, 237.
- [5] F. A. Gallagher, M. I. Kettunen, S. E. Day, D.-E. Hu, J. H. Ardenkjær-Larsen, R. in 't Zandt, P. R. Jensen, M. Karlsson, K. Golman, M. H. Lerche, K. M. Brindle, *Nature* **2008**, 453, 940.

- [6] K.-N. Hu, C. Song, H.-h. Yu, T. M. Swager, R. G. Griffin, *J. Chem. Phys.* **2008**, *128*, 052302.
- [7] C. T. Farrar, D. A. Hall, G. J. Gerfen, S. J. Inati, R. G. Griffin, *J. Chem. Phys.* **2001**, *114*, 4922.
- [8] M. Goldman, *Appl. Magn. Reson.* **2008**, *34*, 219.
- [9] D. S. Wollan, *Phys. Rev. B* **1976**, *13*, 3671.
- [10] D. S. Wollan, *Phys. Rev. B* **1976**, *13*, 3686.
- [11] K. Hu, H. Yu, T. Swager, R. Griffin, *J. Am. Chem. Soc.* **2004**, *126*, 10844.
- [12] C. Song, K. Hu, C. Joo, T. Swager, R. Griffin, *J. Am. Chem. Soc.* **2006**, *128*, 11385.
- [13] T. Fujita, T. Yoshioka, N. Soma, *J. Polym. Sci. Polym. Lett. Ed.* **1978**, *16*, 515.
- [14] A. Pines, M. G. Gibby, J. S. Waugh, *J. Chem. Phys.* **1972**, *56*, 1776.
- [15] S. R. Hartmann, E. L. Hahn, *Phys. Rev.* **1962**, *128*, 2042.
- [16] T. Iijima, *Cryobiology* **1998**, *36*, 165.
- [17] A. Baudot, L. Alger, P. Boutron, *Cryobiology* **2000**, *40*, 151.
- [18] M. Bennati, C. Farrar, J. Bryant, S. Inati, V. Weis, G. Gerfen, P. Riggs-Gelasco, J. Stubbe, R. Griffin, *J. Magn. Reson.* **1999**, *138*, 232.
- [19] A. Schweiger, G. Jeschke, *Principles of pulse electron paramagnetic resonance*, Oxford University Press, Oxford, **2001**.
- [20] Y. S. Lebedev, O. Y. Grinberg, A. A. Dubinskii, O. G. Poluektov in *Bioactive Spin Labels* (Ed.: R. Zhdanov), Springer, Heidelberg, **1992**, p. 227.
- [21] L. R. Becerra, G. J. Gerfen, B. F. Bellew, J. A. Bryant, D. A. Hall, S. J. Inati, R. T. Weber, S. Un, T. F. Prisner, A. E. McDermott, K. W. Fishbein, K. Kreischer, R. J. Temkin, D. J. Singel, R. G. Griffin, *J. Magn. Reson. Ser. A* **1995**, *117*, 28.
- [22] G. J. Gerfen, L. R. Becerra, D. A. Hall, R. G. Griffin, R. J. Temkin, D. J. Singel, *J. Chem. Phys.* **1995**, *102*, 9494.
- [23] L. Becerra, G. Gerfen, R. Temkin, D. Singel, R. Griffin, *Phys. Rev. Lett.* **1993**, *71*, 3561.
- [24] V. L. Granatstein, R. K. Parker, C. M. Armstrong, *Proc. IEEE* **1999**, *87*, 702.
- [25] T. Maly, J. Bryant, D. Ruben, R. Griffin, *J. Magn. Reson.* **2006**, *183*, 303.